The study on dynamic properties of monolithic ball end mills with various slenderness

Szymon Wojciechowski[1,*], *Maciej* Tabaszewski[1], *Grzegorz M.* Krolczyk[2], and *Radosław W.* Maruda[3]

[1] Poznan University of Technology, Faculty of Mechanical Engineering and Management, Institute of Mechanical Technology, Poznan, Poland
[2] Opole University of Technology, 76 Prószkowska St., Opole 45-758, Poland
[3] University of Zielona Gora, 4 Prof. Z. Szafrana street, 65-516 Zielona Gora, Poland

Abstract. The reliable determination of modal mass, damping and stiffness coefficient (modal parameters) for the particular machine-toolholder-tool system is essential for the accurate estimation of vibrations, stability and thus the machined surface finish formed during the milling process. Therefore, this paper focuses on the analysis of ball end mill's dynamical properties. The tools investigated during this study are monolithic ball end mills with different slenderness values, made of coated cemented carbide. These kinds of tools are very often applied during the precise milling of curvilinear surfaces. The research program included the impulse test carried out for the investigated tools clamped in the hydraulic toolholder. The obtained modal parameters were further applied in the developed tool's instantaneous deflection model, in order to estimate the tool's working part vibrations during precise milling. The application of the proposed dynamics model involved also the determination of instantaneous cutting forces on the basis of the mechanistic approach. The research revealed that ball end mill's slenderness can be considered as an important milling dynamics and machined surface quality indicator.

1 Introduction

Ball end milling is usually applied in the production of dies, molds and turbine blades. These processes are very often carried out in finish conditions, thus the high quality of the machined surface is required. Nevertheless, many researches [1-3] show that fundamental problems occurring during ball end milling in finish conditions are the excessive surface roughness and surface location errors, as well as the intense tool wear [22]. The deterioration of surface quality during machining can be attributed to machine tool-cutting process interactions, as: milling kinematics [4, 5], the loss of process stability [6, 23], elastic-plastic deformations of workpiece [7, 8], as well as the tool's working part displacements (vibrations) [9, 10]. Nevertheless, the vibrations seem to be the most influential factor affecting the milling accuracy.

According to Jun et al. [11] and Wojciechowski et al. [12], tool's working part instantaneous displacements during precise milling are significantly affected by the tool deflections induced by cutting forces and machine-toolholder-tool system's geometrical errors (e.g. tool run out). The consequence of the excessive tool displacements during milling are the unacceptable surface errors. Research carried out by Lopez de Lacalle et al. [13] revealed that during finish curvilinear ball end milling of hardened steel, the cutting forces significantly affect the values of surface location errors (SLE). The occurrence of SLE is correlated directly with the tool deflections. Desai and Rao [14] observed that during end milling of curved surfaces, the variation of surface error induced by the tool deflection is not uniform along the tool path. This is mainly due to the change of workpiece curvature along tool path which affects radial engagement of cutting teeth and thereby changing surface error magnitude and the nature of error profile itself. Moreover, during precise milling with relatively low cutting forces or machining with the application of the rigid tools, the geometrical errors of the spindle-toolholder-milling tool system affect influentially the vibrations, and thus the surface quality. According to Sun and Guo [15], the static run out can significantly affect cutter's sweep surface during five-axis flank milling, and thus machined surface's quality. In addition, Buj-Corral et al. [16] developed surface topography model for the peripheral milling with the consideration of machining kinematics, eccentricity and tool geometry. It was noticed that the roughness profiles vary along the work material's height during milling with the occurrence of an eccentricity.

The values of tool deflections generated during machining are correlated directly with the selected cutting parameters (mainly depth of cut, feed per tooth and cutting speed), as well as the dynamical properties of machine-toolholder-tool system. The dynamical properties of this system are very often depended on the selected milling tool's overhang and thus its slenderness. It is well known, that the growth of tool's slenderness causes the growth of its flexibility which can result in an excessive vibrations during milling. However, in many applications, especially in the aerospace industry, the

* Corresponding author: szymon.wojciechowski@put.poznan.pl

need to use long end mills with high length to diameter ratios is necessary. These tools are frequently required for the manufacturing of parts with deep pockets and relatively thin ribs. The researches carried out by Tlusty et al. [17] and Mendes de Aguiar et al. [18] show that the appropriate selection of milling parameters together with the tool slenderness can improve the material removal rate and surface finish. Nevertheless, the direct relations between the ball end mill's slenderness, its dynamical (modal) parameters and the instantaneous tool deflections generated during precise milling are still insufficiently recognized.

This work focuses on the evaluation of dynamical properties of the monolithic ball end mills with various overhangs. The carried out experiments involve the measurements of tool's modal mass, damping and stiffness coefficient, and subsequently the prediction of tool's instantaneous displacements generated during milling, with the application of dynamic model. The obtained results can be further applied to the optimal selection of tool's overhang allowing the minimization of vibrations and improvement in surface finish.

2 Experimental details

2.1 Ball end mill – toolholder system

The analysis of dynamical properties has been conducted on the three ball end mills with various lengths and thus slenderness values (see Tab. 1, Fig. 1). According to López de Lacalle et al. [9], the slenderness of the two-toothed ball end mill can be calculated based on equation:

$$\lambda = \frac{l^3}{(0.8D)^4} \tag{1}$$

The investigated tools, made of cemented carbide with TiAlN coating are intended to finish milling of hardened alloy steels. The tools have been clamped in the hydraulic toolholder. Consequently, the three various overhangs have been obtained.
The selection of hydraulic toolholder was motivated by its relatively high stiffness and damping coefficients, which allow the selection of higher overhangs during milling.

Table 1. Dimensions of ball end mills applied in the research.

Variant	Overhang l [mm]	Diameter D [mm]	Tool length l_c [mm]	Slenderness λ [mm^{-1}]
1	32	10	72	8.8
2	63	10	105	70.2
3	95	10	135	216

According to work [19], the stiffness and damping coefficients of carbide tool-hydraulic toolholder system are respectively 240% and 35% higher than those measured in carbide tool-shrink fit toolholder system.

Fig. 1. Ball end mills and hydraulic toolholder.

2.2 Identification of system's modal parameters

The conducted research involved the evaluation of milling tool-hydraulic toolholder system's dynamical properties, including modal mass m, stiffness coefficient k and damping coefficient c. These quantities have been estimated on the basis of modal test (Fig. 2) enabling the determination of frequency response function (FRF) for the 1 degree of freedom (1 DOF) system.

The FRF function for the 1 DOF system is defined in the following form [20]:

$$H(j\omega) = \frac{X(j\omega)}{F(j\omega)} = \frac{\frac{1}{m}}{-\omega^2 + j\omega\frac{c}{m} + \frac{k}{m}} = \frac{\frac{1}{m}}{-\omega^2 + 2j\omega h + \omega^2_o} \tag{2}$$

where: $H(j\omega)$ is the dynamic compliance, $X(j\omega)$ is system's response in the frequency domain, $F(j\omega)$ is a force in the frequency domain, j – is an imaginary unit, $\omega = 2\pi f$, $2h = c/m$, ω_o is the freqeuncy of free, undamped vibrations.

The applied identification method was based on experimental determination of H_1 characteristics, according to definition:

$$H(j\omega) = H_1(j\omega) = \frac{G_{FX}(j\omega)}{G_{FF}(j\omega)}, \tag{3}$$

where: $G_{FX}(j\omega)$ is a cross spectral density, $G_{FF}(j\omega)$ is auto spectral density.

The experimental stand of modal test (Fig. 2) consisted of impact hammer, 1-directional piezoelectric accelerometer (connected with amplifier), A/D transducer and a PC equipped with software dedicated to the analysis of dynamical properties.

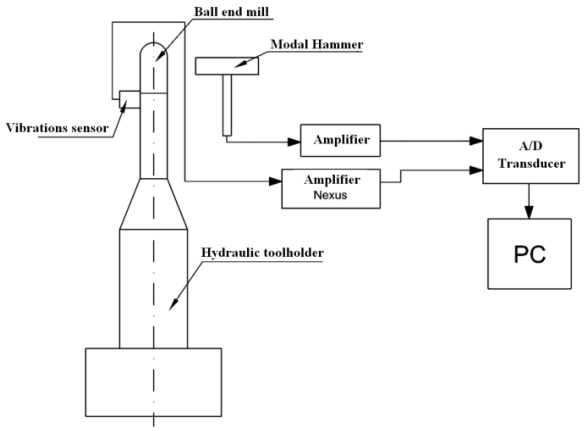

Fig. 2. The scheme of modal test experimental set-up.

The sampling frequency has been selected at the level of 20 480 Hz, and the vibration amplifier's sensitivity was equal to 1 mV/(m/s^2). During the carried out measurements, the maximal acquired system's natural frequency did not exceed the 6000 Hz. Thus, the Nyquist-Shannon criterion, towards the sampling frequency selection has been fulfilled. Moreover, the conducted measurements did not involve the use of filters.

In order to calculate the statistical measures of the acquired signals, the 10-repetitions of measurements for the each investigated variant have been conducted.

2.3 Ball end mill dynamic deflection model

The estimated modal parameters of the ball end mill – toolholder system were further applied in the dynamic deflection model. The instantaneous deflections $y(t)$ of the ball end mill (Fig. 3), induced by cutting forces can be calculated on the basis of the differential motion equation [12]:

$$m \cdot \frac{\mathrm{d}^2 y}{\mathrm{d}t^2} + c \cdot \frac{\mathrm{d}y}{\mathrm{d}t} + k \cdot y(t) = F_z(t) \cdot \sin\alpha + F_y(t) \cdot \cos\alpha \quad (4)$$

where: $y(t)$ – instant tool working part deflection, tangent to the plane defined by the feed motion vector and tool's rotational axis, α – surface inclination angle, $F_z(t)$ – instantaneous force component in the thrust direction, $F_y(t)$ – instantaneous force component in the feed direction.

The equation (4) has been solved numerically in **MATLAB Simulink** software with the application of a variable step Runge-Kutta method (**ode45** solver). The instantaneous values of F_y and F_z forces, can be calculated on the basis of the mechanistic approach, described by equations:

$$F_y(t) = \sum_{j=1}^{z_c} \begin{bmatrix} -\left(K_{re} l_j + K_{rc} A_{zj}\right) \cdot \sin\varphi_{rj} \sin\varphi_j + \\ -\left(K_{ae} l_j + K_{ac} A_{zj}\right) \cdot \cos\varphi_{rj} \cdot \sin\varphi_j + \\ -\left(K_{te} l_j + K_{tc} A_{zj}\right) \cdot \cos\varphi_j \end{bmatrix} \quad (5)$$

$$F_z(t) = \sum_{j=1}^{z_c} \begin{bmatrix} \left(K_{re} l_j + K_{rc} A_{zj}\right) \cdot \cos\varphi_{rj} + \\ -\left(K_{ae} l_j + K_{ac} A_{zj}\right) \cdot \sin\varphi_{rj} \end{bmatrix} \quad (6)$$

where: K_{te}, K_{re}, K_{ae} are the edge specific coefficients, K_{tc}, K_{rc}, K_{ac} are the shear specific coefficients, l_j is the length of cutting edge of the j-th tooth, A_{zj} is the cross sectional area of cut of the j-th tooth, φ_j, φ_{rj} are the instantaneous positioning angles of the j-th cutting edge, z_c is the active number of teeth.

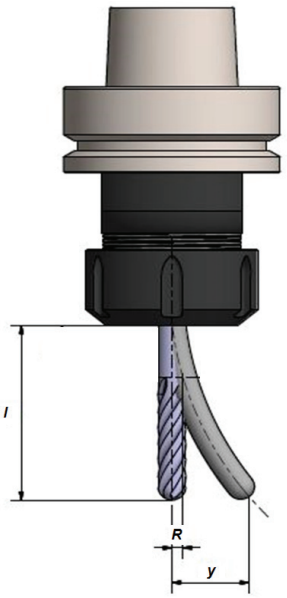

Fig. 3. Ball end mill deflection in the y direction.

In order to calculate the instant cutting forces (F_y, F_z) it is necessary to determine cross sectional area of cut and active length of cutting edge, as well as calibrate specific coefficients. These parameters' values can be estimated with the application of methods and data presented in work [21], which was focused on the cutting forces modeling during ball end milling of hardened alloy steel.

3 Results and discussion

Figures 4 – 7 depict the modal parameters' (k, c, m, f_o) values determined for the investigated tool slenderness values. It can be seen that the growth of tool overhang (and thus the slenderness) causes the monotonic decrease of system's damping coefficient c, stiffness coefficient k and natural frequency f_o. Moreover, the c, k, f_o = f(λ) dependencies are described by the power functions, which means that in a range of higher tool slenderness values ($\lambda \geq 70.2$ mm^{-1}), the differences in modal parameters' values are decreasing and stabilizing. It should be noted, that the decline in c, k, f_o values can be undesirable because it can lead to the growth of tool deflections during milling (induced by the decrease of stiffness coefficient), reduction of process dynamical stability (induced by the decrease of damping coefficient), as well as the higher risk of resonance

phenomenon (induced by the decrease of natural frequency).

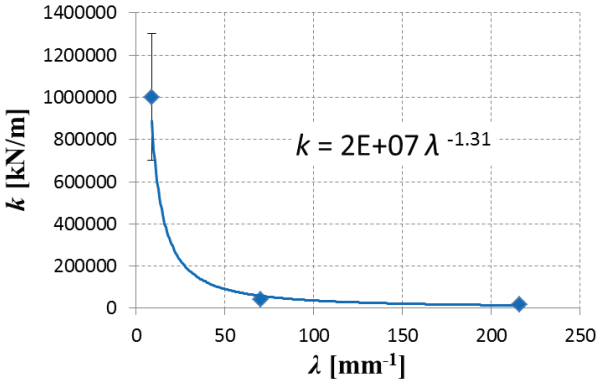

Fig. 4. The influence of the tool slenderness on the system's stiffness coefficient.

Nevertheless, in case of a modal mass m, a non-monotonic influence of tool slenderness value is seen. The lowest m values are reached for the moderate investigated slenderness: λ = 70.2 mm^{-1}. The modal mass is a parameter which describes the mass of the investigated system which is subjected to the deflections induced by the variable force. Thus, the lower modal mass, the lower ball end mill's volume is subjected to the deflections during milling.

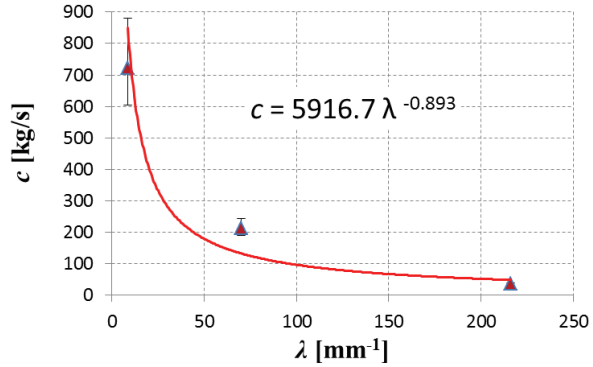

Fig. 5. The influence of the tool slenderness on the system's damping coefficient.

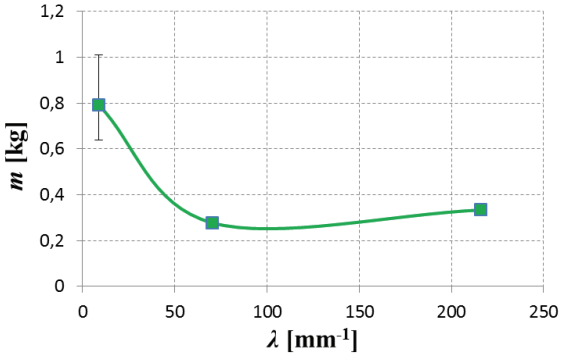

Fig. 6. The influence of the tool slenderness on the system's modal mass.

Figures 4 – 7 show also that the highest error bars' values of the determined m, c, k parameters are reached for the lowest investigated slenderness (which corresponds to highest measured system natural frequency). It can be caused by the relatively low sampling rate (20 480 Hz), which in case of a system with the average natural frequency equaled to 5693 Hz results in approx. 3 measurements per vibration period. Thus, it affects the appearance of some inaccuracies in the obtained digital signal's form.

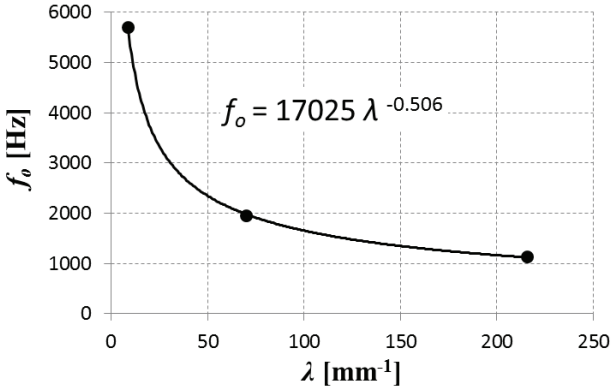

Fig. 7. The influence of the tool slenderness on the system's natural frequency.

The next step of analysis involved the simulations of ball end mill's working part instantaneous deflections $y(t)$. During this stage, the upper recommended cutting parameters' values for the precise milling of hardened steel have been selected as: a_p = 0.3 mm and f_z = 0.1 mm/tooth. Figures 8-10 show that independently on the investigated system, the instantaneous deflections reach alternately the positive and negative values, which indicates that the tool's working part is periodically indenting inside the workpiece, (exceeding the nominal depth of cut value), as well as moving outside the material which is being cut (reducing the nominal depth of cut value).

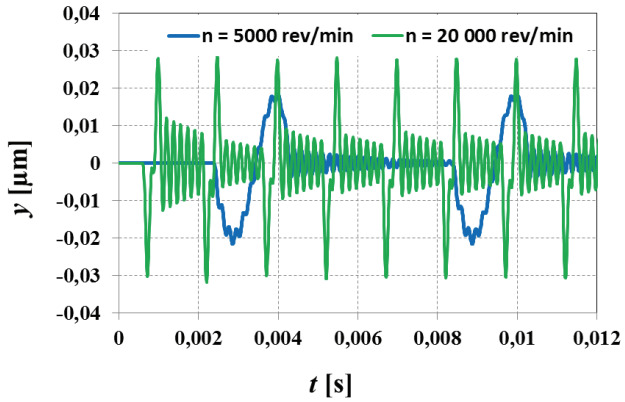

Fig. 8. The time course of instantaneous tool deflections for λ = 8.8 mm^{-1}.

In case of the system with the lowest slenderness (λ = 8.8 mm^{-1}), the deflection amplitudes are not exceeding the 0.04 µm, independently on the selected rotational speed, which means that they have insignificant contribution to the formation of surface finish, even during the precise milling. Nevertheless, in case of the moderate tool overhang (λ = 70.2 mm^{-1}), the

deflection amplitudes are significantly higher and reach almost 2 µm for the n = 20 000 rev/min and 0.5 µm when the n = 5 000 rev/min. It is worth indicating that further growth of tool overhang/slenderness is not affecting influentially the growth of tool deflection amplitudes. In case of the system with the highest investigated overhang/slenderness, the deflection amplitudes are lower than 3 µm for the n = 5 000 rev/min and 2 µm when the n = 20 000 rev/min. This finding reveals that in a range of a higher rotational speeds, the deflection amplitudes are similar for the systems with λ = 70.2 mm^{-1} and λ = 216 mm^{-1}. Nevertheless, when the system with λ = 216 mm^{-1} is applied, the forced vibrations reach the steady state after longer cutting time (~0.03 s), in comparison to milling conducted with less slender systems ($\lambda \leq$ 70.2 mm^{-1}).

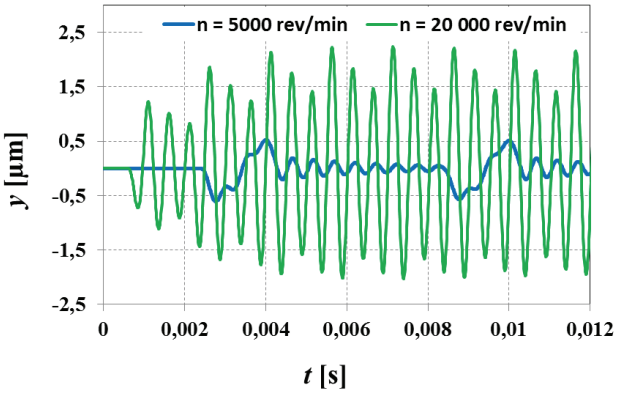

Fig. 9. The time course of instantaneous tool deflections for λ = 70.2 mm^{-1}.

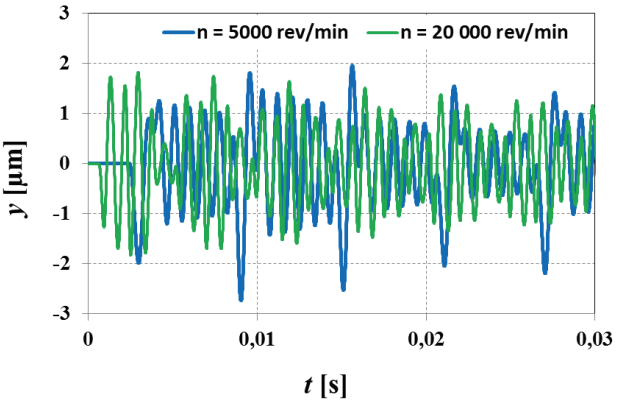

Fig. 10. The time course of instantaneous tool deflections for λ = 216 mm^{-1}.

It should be noted that instantaneous tool y deflections with the relatively high frequencies (higher than tooth passing frequency – $f_t = (zn)/60$), found for the systems with λ = 70.2 mm^{-1} and λ = 216 mm^{-1} can contribute to the formation of surface roughness profile in the direction perpendicular to the feed motion vector.

Figures 8-10 reveal also that system's slenderness value affect the relations between the maximal tool deflections and the selected rotational speed. In case of systems with $\lambda \leq$ 70.2 mm^{-1}, the growth of rotational speed induces the growth of deflection amplitudes, however the opposite trend is seen in case of a system with the highest investigated slenderness (λ = 216 mm^{-1}). These relations are strictly correlated with the superposition of forced vibrations dominant harmonic's frequency to the system's natural frequency. In case of systems with $\lambda \leq$ 70.2 mm^{-1}, the growth of rotational speed causes that the ratio of forced vibration dominant harmonic's frequency to system's natural frequency aims at 1. Thus it contributes to the growth of vibrations amplitudes – according to the resonance curve. Nevertheless, in case of a system with λ = 216 mm^{-1}, for the higher rotational speed value (n=20 000 rev/min), the ratio of forced vibration dominant harmonic's frequency to system's natural frequency is greater than 1. Consequently, it contributes to the decline of vibration amplitude during milling with the higher rotational speed.

4 Conclusions

On the basis of the carried out research the following conclusions have been formulated.

- The growth of tool overhang (slenderness) causes the monotonic decrease of system's damping coefficient c, stiffness coefficient k and natural frequency f_o, described by the power functions. However, in case of a modal mass m, a non-monotonic influence of tool overhang is seen.
- The application of the ball end mill with slenderness of λ = 216 mm^{-1} can cause almost 75-fold growth of vibration amplitude in relation to system with λ = 8.8 mm^{-1}. On the other side, the simulated maximal tool deflections are not exceeding 3 µm, independently on the investigated tool slenderness. This suggests that ball end mills with overhangs in a range from the 32 mm to 95 mm, clamped in the hydraulic toolholder can be applied during precise milling of hardened steel. However, the vibrations generated during the milling process can be affected also by the machine-toolholder-tool geometrical errors (e.g. run out).
- Simulations based on the solution of differential motion equation reveal also that system's slenderness value affect the relations between the maximal tool deflections and the selected rotational speed. In case of systems with $\lambda \leq$ 70.2 mm^{-1}, the growth of rotational speed induces the growth of deflection amplitudes, however the opposite trend is seen in case of system with the highest investigated slenderness (λ = 216 mm^{-1}). This finding suggests that tools with higher overhangs can be applied during precise milling in HSM conditions. Nevertheless, the forced vibrations dominant harmonic's frequency should be higher than the system's natural frequency.

References

1. Y. Pan, Y. Changfeng, X. Shaohua, Z. Dinghua, D. Xingtang, Procedia CIRP **56** (2016)

2. M.A. Salgado, L.N. Lopez de Lacalle, A. Lamikiz, J. Munoa, J.A. Sanchez, Int. J. Mach. Tools Manuf. **45**, 6 (2005)
3. G.M. Kim, B.H. Kim, C.N. Chu, Int. J. Mach. Tools Manuf. **43** (9) (2003)
4. S. Wojciechowski, P. Twardowski, M. Wieczorowski, Metrol. Meas. Syst. **21** (1) (2014)
5. S. Wojciechowski, P. Twardowski, M. Pelic, R.W. Maruda, S. Barrans, G. Krolczyk, Precis Eng. **46** (2016)
6. E. Ozturk, E. Budak, J. Manuf. Sci. Eng. **132** (2), (2010)
7. Schultheiss F., Hagglund S., Bushlya V., Zhou J., Stahl J-E, Procedia CIRP **13** (2014)
8. S. Wojciechowski, R.W. Maruda, P. Nieslony, G.M. Krolczyk, International Int. J. Mech. Sci. **119** (2016)
9. L.N. López de Lacalle, A. Lamikiz, J.A. Sanchez, M.A. Salgado, Int. J. Adv. Manuf. Technol. **24** (2004)
10. S. Wojciechowski, P. Twardowski, M. Pelic, Procedia CIRP **14** (2014)
11. M.B.G. Jun, R.E. DeVor, S.G. Kapoor, J. Manuf. Sci. Eng.-Trans. ASME **128** 2006
12. S. Wojciechowski, T. Chwalczuk, P. Twardowski, G.M. Krolczyk, Arch. Civ. Mech. Eng. **15**, 4, (2015)
13. L.N. López de Lacalle, A. Lamikiz, J.A. Sanchez, M.A. Salgado, Int. J. Mach. Tools Manuf. **47** (2007)
14. K.A. Desai, P.V.M. Rao, J. Mater. Process. Technol. **212** (2012)
15. Y. Sun, Q. Guo, J. Manuf. Sci. Eng.-Trans. ASME **134** (2012)
16. I. Buj-Corral, J. Vivancos-Calvet, H. Gonzalez-Rojas, Int. J. Mach. Tools Manuf. **51** (2011)
17. J. Tlusty, S. Smith, W.R. Winfough, CIRP Ann-Manuf. Technol. **45** (1996)
18. M. Mendes de Aguiar, A.E. Diniz, R. Pederiva, Int. J. Mach. Tools Manuf. **68** (2013)
19. Z. Nowakowski, S. Wojciechowski, Mechanik **08/09** (2015)
20. S. Gade, H. Herlusfen, Technical Review, **2**, Bruel & Kjear A/S (1994)
21. S. Wojciechowski, Int. J. Mach. Tools Manuf., **89** (2015)
22. J. Kuczmaszewski, P. Pieśko, Eksploat. Niezawodn. **16**(1) (2014)
23. R. Rusinek, M. Wiercigroch, P. Wahi, Procedia CIRP **31** (2015)